


# Stabilization of the Time-Dependent Drift-Diffusion Model for Fermi-Dirac Statistics

1<sup>st</sup> Tobias Linn

Chair of Electromagnetic Theory  
RWTH Aachen University  
Aachen, Germany

 0000-0002-7681-7725


2<sup>nd</sup> Jan Flasskamp

Chair of Electromagnetic Theory  
RWTH Aachen University  
Aachen, Germany

 0009-0000-4600-1226

3<sup>rd</sup> Christoph Jungemann

Chair of Electromagnetic Theory  
RWTH Aachen University  
Aachen, Germany

 0000-0002-3423-4046

**Abstract**—The Scharfetter-Gummel scheme is a widely used stabilization method for solving the drift-diffusion model. However, it is only applicable when using Maxwell-Boltzmann carrier statistics and does not yield thermodynamically consistent results in other cases, such as Fermi-Dirac statistics. Several modifications to the scheme have been proposed as improvements in this case such as Diffusion enhanced schemes. These are usually based on approximations which are not always accurate. Using similar assumptions as Scharfetter and Gummel, we develop a new scheme where the boundary value problem for each edge is solved with the shooting method and a high-order solver for ordinary differential equations. Even though the computational cost is much larger than for the original scheme, it can be effectively parallelized and a significantly negative impact on the total runtime is avoided. The scheme is applied to an NMOSFET device and stationary, transient and small-signal solutions at cryogenic temperatures are presented.

**Index Terms**—drift-diffusion model, numerical stability, cryogenics

## I. INTRODUCTION

The drift-diffusion model (DDM) is the basis of technology computer aided design (TCAD) and thus of today's industrial device design process despite its shortcomings[1]. This is due to the unrivaled numerical robustness of the DDM, when the Scharfetter-Gummel stabilization scheme is used in conjunction with a finite volume discretization in the non-degenerate case [2]. For a certain class of mobility and generation-recombination models it can be shown that the discrete DDM has a unique positive solution (e.g. [3], [4]). Furthermore, these properties improve the convergence when solving the nonlinear equation system.

Unfortunately, the Scharfetter-Gummel stabilization does not work in the case of a degenerate particle gas, and a similar simple stabilization scheme does not exist. While in many applications degeneracy can be ignored, this is no longer the case, if, for example, the temperature is reduced (e.g. control logic for quantum computing), and Fermi-Dirac statistics have to be used. This modifies the diffusion term in the DDM, it is no longer possible to separate the impact of the electrostatic potential from the quasi-Fermi-level in the Fermi-Dirac integral for the particle density, and Slotboom variables can not be derived. Various modifications of the Scharfetter-Gummel stabilization for the degenerate case have been developed, which are based on certain approximations

introducing their own problems [5]. Koprucki and Gärtner developed a new approach, where they use similar approximations as Scharfetter and Gummel for the current along an edge of the Delaunay grid and solve the resultant nonlinear integral equation by numerical means [6].

Instead, here we solve the corresponding boundary value problem numerically under the same assumptions as Scharfetter and Gummel, which ensures consistency with the original stabilization in the case of low (non-degenerate) particle densities. We use the shooting method together with the adaptive RADAU5 ODE solver, where the accuracy of the solution can be controlled [7].

## II. METHOD

The electron and hole current densities are assumed to be constant along an edge and are given by

$$J_n = -\frac{e\mu_n}{\Delta x} n \frac{\partial \Phi_n}{\partial x} \quad \text{and} \quad J_p = \frac{e\mu_p}{\Delta x} p \frac{\partial \Phi_p}{\partial x} \quad (1)$$

where  $e$  is the elementary charge,  $\mu_{n/p}$  the electron/hole mobility,  $n/p$  the electron/hole density and  $\Phi_{n/p}$  the electron/hole quasi-fermi potential.  $\Delta x$  is the edge length and  $x \in [0, 1]$  the normalized edge coordinate. The relationship between the density and the corresponding quasi-fermi potential is

$$n = N_C F_{1/2} \left( \frac{\varphi - \Phi_n}{V_T} - \frac{E_C}{k_B T} \right) = N_C F_{1/2}(\eta_n) \quad (2)$$

$$p = N_V F_{1/2} \left( \frac{\Phi_p - \varphi}{V_T} + \frac{E_V}{k_B T} \right) = N_V F_{1/2}(\eta_p), \quad (3)$$

where  $N_{C/V}$  is the effective density of states for the conduction and valence band,  $T$  is the temperature,  $k_B$  the Boltzmann constant and  $V_T = \frac{k_B T}{e}$  the thermal voltage.  $F_{1/2}(\eta)$  is the Fermi-Dirac integral where  $\eta_{n/p}$  are the dimensionless chemical potentials. Assuming that the electrostatic potential varies linearly along the edge, the ODE in equation eq. (1) can be reformulated as

$$\frac{\partial \eta}{\partial x} = \Delta \varphi - \frac{j}{F_{1/2}(\eta)} \quad (4)$$

with the normalized potential difference  $\Delta \varphi = -q \frac{\varphi_R - \varphi_L}{V_T}$ , where  $q = -1$  for electrons and  $q = +1$  for holes and  $\varphi_{L/R}$  is the potential at the left and right end of the edge.

The normalized current density is  $j = -\frac{q\Delta x}{k_B T N_C / \sqrt{m_n/p}} J_{n/p}$ . For the sake of brevity, in the following only electrons are considered.

The goal is to calculate  $j$  for a given  $\Delta\varphi$  under the assumption that

$$\begin{aligned}\eta(x=0) &= \eta_L = F_{1/2}^{-1}\left(\frac{n_L}{N_C}\right) \\ \eta(x=1) &= \eta_R = F_{1/2}^{-1}\left(\frac{n_R}{N_C}\right).\end{aligned}\quad (5)$$

To that end we take an initial guess for the value of  $j$  and solve eq. (4) numerically, e.g. starting from  $\eta_L$  at  $x=0$  going to  $x=1$ . The difference between the resulting  $\tilde{\eta}_R = \eta(x=1)$  and  $\eta_R$  is then brought to zero by changing  $j$  until the correct value is found. This is achieved by means of a Newton iteration, where the update for the  $n$ -th step is calculated by

$$j_{k+1} = j_k - \left(\frac{\partial \tilde{\eta}_R}{\partial j}\bigg|_{j_k}\right)^{-1} \left(\tilde{\eta}_R\bigg|_{j_k} - \eta_R\right). \quad (6)$$

We use a custom implementation of the RADAU5 solver that will not only give us the value  $\tilde{\eta}_R$  but also its derivative. The stepsize is adaptively changed to ensure that the accuracy of the solution is close to machine precision, which is necessary for the Newton iteration to converge. The RADAU5 solver is based on a fully implicit Runge-Kutta scheme of type Radau IIA. It has fifth-order accuracy and is L-stable, which is advantageous as depending on the parameters the ODE might be quite stiff.

At first glance eq. (4) looks fairly simple, however, under certain conditions the ODE solver might not be able to achieve a solution due to numerical reasons. This is especially the case for small values of  $\eta$ , resulting in huge values for  $\frac{j}{F_{1/2}(\eta)}$ . On the other hand, in that case the Fermi-Dirac integral can be approximated very accurately. We use

$$F_{1/2}(\eta) \approx \exp(\eta) \quad \text{for } \eta < -36 \quad (7)$$

and

$$F_{1/2}(\eta) \approx \frac{1}{\gamma + \exp(-\eta)} \quad \text{for } -36 \leq \eta \leq -16 \quad (8)$$

with  $\gamma = \sqrt{\frac{1}{8}} \approx 0.35$ . Note that the approximation in eq. (8) is similar to the one by Blakemore [8] who used  $\gamma = 0.27$ , however within that interval our value is more accurate. In fact, both eqs. (7) and (8) are exact when using double precision arithmetic. If  $\eta$  is not small we use the implementation by Fukushima [9].

If both  $\eta_{L/R} < -36$ , the regular Schafetter-Gummel result is obtained, while for  $\eta_{L/R} < -16$  a similar iteration scheme as in [5] can be used. If only one of the two boundary values for  $\eta$  is small, the edge can be split at the point where  $\eta = -16$ , and the region where  $\eta < -16$  is analytically integrated.

In the following we assume w.l.o.g. that  $\Delta\varphi \leq 0$ , which can always be achieved by reversing the edge direction if necessary. We can identify two cases where the solution to the ODE results in a linear  $\eta(x)$ , first if  $\Delta\eta = \eta_R - \eta_L \approx 0$  and second

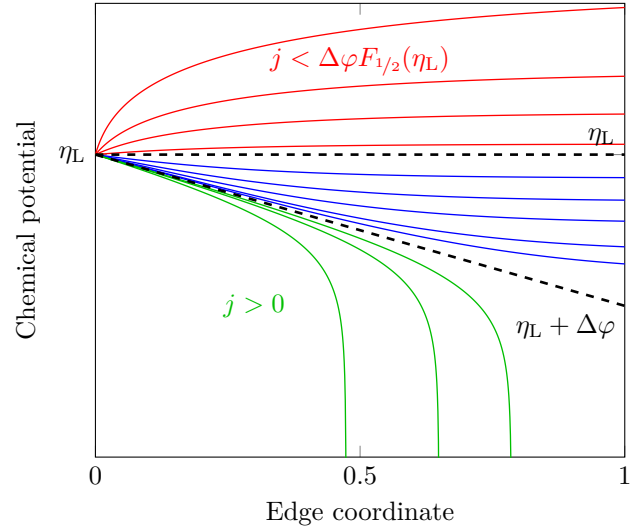


Fig. 1:  $\eta(x)$  for  $\Delta\varphi < 0$  starting from  $\eta_L$  and going from left to right for different values of  $j$ .

if  $\Delta\eta \approx \Delta\varphi$ . In the first case, we write  $\eta(x) = \eta_L + \delta\eta(x)$  and  $j = \Delta\varphi F_{1/2}(\eta_L) + \delta j$  with  $\delta\eta(x)$  and  $\delta j$  small, and linearize the ODE:

$$\frac{\partial \delta\eta}{\partial x} = -\frac{\delta j}{F_{1/2}(\eta_L)} + \Delta\varphi \frac{F_{-1/2}(\eta_L)}{F_{1/2}(\eta_L)} \delta\eta. \quad (9)$$

The solution can then be carried out analytically resulting in

$$j = F_{1/2}(\eta_L)(\Delta\varphi - \Delta\eta)B\left(\Delta\varphi \frac{F_{-1/2}(\eta_L)}{F_{1/2}(\eta_L)}\right) \quad (10)$$

where  $B(x) = \frac{x}{\exp(x)-1}$  is the Bernoulli function. In the second case the current density is small, and a similar strategy yields

$$j = \overline{F_{1/2}(\eta)}(\Delta\varphi - \Delta\eta) \quad (11)$$

where

$$\overline{F_{1/2}(\eta)} = \left(\int_{\eta_L}^{\eta_R} \frac{1}{F_{1/2}(\eta)} d\eta\right)^{-1} \quad (12)$$

is the harmonic mean of the normalized density over the edge. It is calculated by gaussian quadrature.

For the remaining cases the ODE solver is used. Depending on the direction and on the values of  $\eta_{L/R}$  and  $\Delta\varphi$ , the solution might exponentially increase with  $x$ . To avoid numerical over- and underflows, we therefore always choose the direction along which the exponential term decreases. In Fig. 1 the solution of eq. (4) is shown for a fixed value of  $\eta_L$  and different values of  $j$ . There are three different cases that can be identified: The first case (red) is that  $\eta_R > \eta_L$  which corresponds to  $j < \Delta\varphi F_{1/2}(\eta_L)$ . The second case (blue) is obtained for  $\eta_L < \eta_R < \eta_L + \Delta\varphi$  and corresponds to  $\Delta\varphi F_{1/2}(\eta_L) < j < 0$ . In these two cases the ODE is solved from the left to the right, as  $\eta(x)$  does not increase exponentially. Only in the third case (green) with  $\eta_R < \eta_L + \Delta\varphi$  and  $j > 0$  we solve the ODE from the right to the left.

To stabilize the Newton iteration, we always maintain a

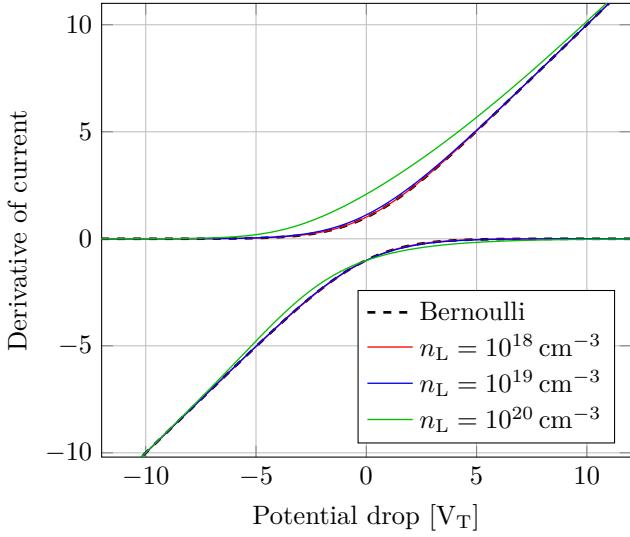


Fig. 2: Bernoulli coefficients and corresponding normalized derivatives of the current w.r.t. the density for the degenerate case at the left and right grid nodes. The particle density at the right-hand side of the edge is fixed to  $n_R = 10^{18} \text{ cm}^{-3}$ .

lower and upper limit for  $j$  with  $j_{\min} < j < j_{\max}$ . These are updated during the iteration based on the sign of the residual. If the Newton update violates this condition, a simple bisection step is used instead, which guarantees convergence. The previously given initial bounds for  $j$  depending on the case can be improved if we require that at some point along the edge the slope of  $\eta(x)$  must be exactly equal to  $\Delta\eta$ . This leads to

$$j_{\min} = \max(j_{\min,0}, \min(n_L, n_R)|\Delta\varphi - \Delta\eta|) \quad (13)$$

$$j_{\max} = \min(j_{\max,0}, \max(n_L, n_R)|\Delta\varphi - \Delta\eta|). \quad (14)$$

Once the Newton iteration is converged, the derivatives of the solution  $j$  with respect to  $\eta_{L/r}$  and  $\Delta\varphi$  are obtained by implicit differentiation.

### III. RESULTS

The obtained edge current density together with its derivatives with respect to the particle densities and electrostatic potentials at both ends of the edge are sufficient to solve the continuity equation discretized by the finite volume method with an outer Newton iteration. At this level no differences compared to the standard DDM occur. Since the currents on the grid edges depend only on local variables, they can be evaluated in parallel. Furthermore, the number of edges is linear in the number of grid nodes and in the 2D or 3D cases the additional workload compared to the standard DDM is quite manageable (about 1.5 to 2.0 times slower in the case of our 2D example).

The Bernoulli coefficients of the non-degenerate case correspond to the normalized derivatives of the current w.r.t. the densities (Fig. 2). In the case of low densities or large potential drops the Bernoulli coefficients are reproduced. Furthermore,

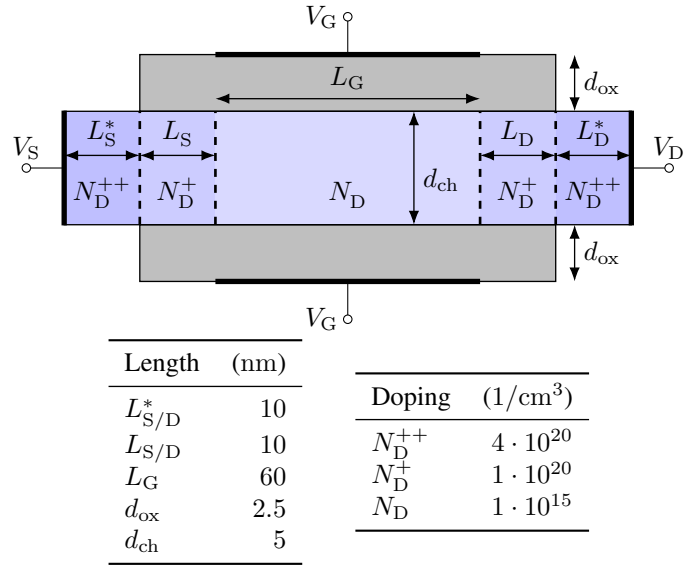


Fig. 3: Double-gate NMOSFET device with relevant parameters.

the coefficients have the same sign as the Bernoulli coefficients, which is a prerequisite for numerical stability. For zero bias (equilibrium) the current vanishes and the DDM particle density equals the one calculated directly by Fermi-Dirac statistics.

The stabilization scheme is tested for a double gate NMOSFET which is shown in Fig. 3, where we assume a constant mobility of  $\mu = 100 \text{ cm}^2/(\text{V s})$ . Note that the specific value is rather unimportant, since our goal is only to demonstrate the numerical stability of our scheme, and not to produce physically meaningful results. We use partial ionization in conjunction with a simple generation/recombination model [10].

In Fig. 4 the output characteristics at 4 K are shown, and no numerical problems are encountered. The self-consistent Newton-Raphson method converges quadratically and the final change in the potential is less than  $10^{-12} \text{ V}$ , demonstrating that the global solution accuracy is not negatively affected by the ODE solver.

The approach also works in the transient case, and in Fig. 5 the terminal currents are shown when the device is turned on at 0 ps. The transient simulation is numerically very robust, although the drain/source bias is almost 3000 times the thermal voltage at this low temperature. The simulation is performed using the TR-BDF2 method [11] with adaptive time stepping.

Admittance parameters are shown in Fig. 6, so all usual simulation modes (stationary, small-signal and large-signal) are possible.

In conclusion, we have demonstrated that the DDM based on Fermi-Dirac statistics can be solved in a numerically robust way at low temperatures without a significant CPU time penalty. Furthermore, this approach should also work in the case of a hydrodynamic model.

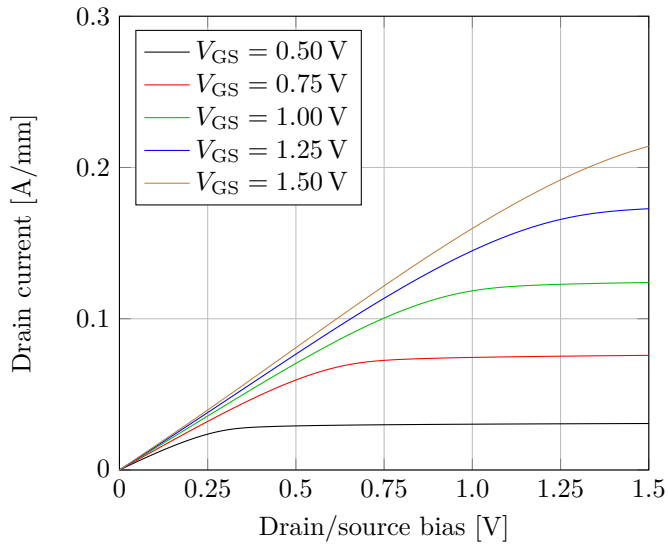


Fig. 4: Output characteristics of the double gate NMOSFET at 4 K.

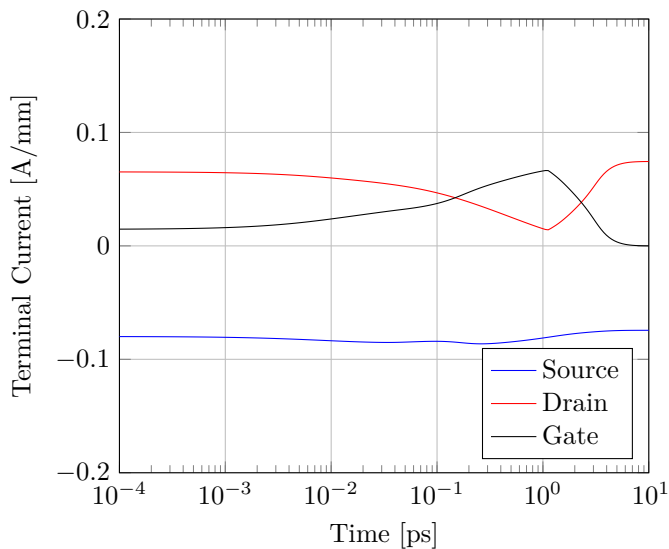


Fig. 5: Transient results for an abrupt turn-on of the NMOSFET at 4 K,  $V_{GS} = 0.2 \text{ V} \rightarrow 0.75 \text{ V}$ , and  $V_{DS} = 0 \text{ V} \rightarrow 1.0 \text{ V}$ .

#### REFERENCES

[1] M. A. Stettler, S. M. Cea, S. Hasan, L. Jiang, P. H. Keys, C. D. Landon, P. Marepalli, D. Pantuso, and C. E. Weber, "Industrial tcad: modeling atoms to chips," *IEEE Transactions on Electron Devices*, vol. 68, no. 11, pp. 5350–5357, 2021.

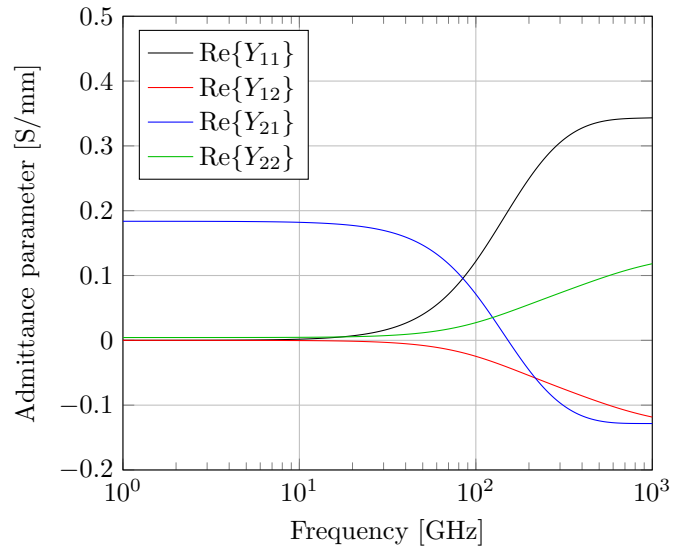


Fig. 6: Admittance parameters of the NMOSFET at 4 K,  $V_{GS} = 0.75 \text{ V}$ , and  $V_{DS} = 1.0 \text{ V}$  in common-source configuration.

- [2] D. L. Scharfetter and H. K. Gummel, "Large-signal analysis of a silicon read diode oscillator," *IEEE Transactions on electron devices*, vol. 16, no. 1, pp. 64–77, 1969.
- [3] J. W. Slotboom, "Computer-aided two-dimensional analysis of bipolar transistors," *IEEE Transactions on Electron Devices*, vol. 20, no. 8, pp. 669–679, 1973.
- [4] B. Meinerzhagen and C. Jungemann, *Spherical Harmonics Expansion and Multi-Scale Modeling*. Cham: Springer International Publishing, 2023, pp. 1413–1450.
- [5] T. Koprucki and K. Gärtner, "Discretization scheme for drift-diffusion equations with strong diffusion enhancement," *Optical and Quantum Electronics*, vol. 45, no. 7, pp. 791–796, 2013.
- [6] P. Farrell, M. Patriarca, J. Fuhrmann, and T. Koprucki, "Comparison of thermodynamically consistent charge carrier flux discretizations for fermi-dirac and gauss-fermi statistics," *Optical and Quantum Electronics*, vol. 50, no. 2, p. 101, Feb 2018.
- [7] G. Wanner and E. Hairer, *Solving ordinary differential equations II*. Springer Berlin Heidelberg, 1996.
- [8] J. Blakemore, "Approximations for fermi-dirac integrals, especially the function  $f_{1/2}(\eta)$  used to describe electron density in a semiconductor," *Solid-State Electronics*, vol. 25, no. 11, pp. 1067–1076, 1982.
- [9] T. Fukushima, "Precise and fast computation of fermi-dirac integral of integer and half integer order by piecewise minimax rational approximation," *Applied Mathematics and Computation*, vol. 259, pp. 708–729, 2015.
- [10] S. M. Sze, *Physics of Semiconductor Devices*. New York: Wiley, 1981.
- [11] R. Bank, W. Coughran, W. Fichtner, E. Grosse, D. Rose, and R. Smith, "Transient simulation of silicon devices and circuits," *IEEE Transactions on Computer-Aided Design of Integrated Circuits and Systems*, vol. 4, no. 4, pp. 436–451, 1985.